



Influence of Fault Current Limiter in Voltage Drop and TRV Considering Wind Farm

Sajjad Dadfar^{1*}, Mohammad Mahdi Marzban²

¹Ministry of Energy, IRAN Power Generation Transmission and Distribution Management Company (TAVANIR), Tehran, Iran

²Ministry of Energy, Thermal Power Plants Holding Company (TPPH), Tehran, Iran, m.marzban@tpph.ir

Abstract

Influence of distributed generation systems in the distribution systems can increase the level of short-circuit current. The effectiveness of distributed generation systems is affected by the size, location, type of distributed generation systems technology, and the methods of connecting to distribution systems. Wind turbine system is the examples of distributed generation source. Not only does the using of fault current limiter reduce the pressure on network equipment, but also it can provide a connection to improve the function of the system. There are different types of superconducting fault current limiter, which are made of various superconducting materials and with different designs. Superconducting fault current limiter can be categorized as resistive, inductive and bridge. In this research, the effect of superconducting fault current limiter factors investigated on transient recovery voltage, voltage drop and transient behavior of wind turbine systems based on fixed speed wind turbines, in order to study the behavior of all three types of superconducting fault current limiter that was installed in distributed generation systems. The simulation results show that the transient recovery voltage, the voltage drop and the transient behavior of fixed speed wind turbines have been improved using superconducting fault current limiter.

Keywords: SFCL; TRV; FSWT; Voltage drop; Circuit breaker

Article history: Received 28-FEB-2018; Revised 12-MAR-2018; Accepted 26-MAR-2018.

© 2018 IAUCTB-IJSEE Science. All rights reserved

1. Introduction

In this paper, the protection coordination of the protective devices with a Superconducting Fault Current Limiter (SFCL) due to the DG's application location in a power distribution system was analyzed as the typical application location of the Distributed Generation (DG) in a power distribution system, the bus line, the middle point of the fault feeder and the middle point of the sound feeder were considered.

In case that the DG was applied into the middle point of the fault feeder, the current flowing into the drawing point of the fault feeder during the fault period was seen to be decreased, which caused the lower resistance generation of the SFCL and thus, prevented the lock-out operation of the R/C from being delayed. On the other hand, the lock-out operation of the R/C in case that the DG was applied into the middle point of the sound feeder could be analyzed to be relatively quickly completed due to the larger feeder current in spite of the larger resistance generation of the SFCL [1].

In this paper, through the short-circuit tests for the simulated power distribution system; the protection coordination of the protective devices with a SFCL due to the DG introduction into a power distribution system was analyzed. The resistance, as the design parameter of the SFCL, was considered and the design condition of the SFCL to improve the protection coordination of the protective devices considering the DG introduction in a power distribution system was described from the analysis on the short-circuit tests through the adjustment of the shunt resistance of the SFCL[2].

In this paper, multiple criteria such as the number of SFCLs, fault current reduction, and the total operating time of the relays are considered in determining the optimal placement of SFCLs for protection of an electric power systems with DGs. An EM-based method is proposed to select the weight for each criterion and is used in conjunction with scenario optimization to sequentially solve the scenario subproblem and the tracking problem in

the multi-criteria SFCL placement problem. The numerical results show that SFCL placement determined by the proposed method can help reduce the fault current to within the breaking capacity of the protective devices while meeting the CTI requirements of the relays [3]. In this paper, the application of the active SFCL into a power distribution network with DG units is investigated. For the power frequency overvoltage caused by a single-phase grounded fault, the active SFCL can help to reduce the overvoltage's amplitude and avoid damaging the relevant distribution equipment. The active SFCL can as well suppress the short-circuit current induced by a three-phase grounded fault effectively, and the power system's safety and reliability can be improved.

Moreover, along with the decrease of the distance between the fault location and the SFCL's installation position, the current-limiting performance will increase. In recently years, more and more dispersed energy sources, such as wind power and photovoltaic solar power, are installed into distribution systems. Therefore, the study of a coordinated control method for the renewable energy sources and the SFCL becomes very meaningful, and it will be performed in future [4]. The paper compared the resistive type and flux-lock type SFCLs regarding their working principles, fault current limitations, current flowing into the High Temperature Superconducting (HTS) element and their impacts on maintaining DG voltage at different locations.

Simulation results in PSCAD/EMTDC indicate that both types of SFCL are able to significantly reduce the fault current. The resistive SFCL performs better at limiting the peak current due to its shorter fault detection time and smaller decay time constant of fault current DC component. However, full load current will flow through the HTS coil of the resistive SFCL under nominal operation. Hence the flux-lock type SFCL is more suitable for system expansion, for the reason that only a specific proportion of load current will flow through the HTS thin film. In terms of voltage dip management and DG mechanical speed stability enhancement, the results imply that SFCLs at both locations can provide terminal voltage improvement for the Doubly Fed Induction Generator (DFIG) based wind turbine. SFCL deployed between DG and network is able to protect the DG from any external fault in the test system.

By contrast, the presence of SFCL at Location II can only protect the DG from the fault occurred on the branch with SFCL. Compared with flux-lock SFCL, the resistive type is more suitable to be installed at DG terminal since it has no stability

issues with large enough shunt resistance. However, the voltage deviation during superconductor recovery time needs to be considered in future studies [5].

The impact of fault-current-limiting devices on safety and power quality of distribution networks has been quantitatively investigated. The thermal let-through related to actual short circuit current waveforms rather than the rms value of the symmetric component was introduced for assessing the potential impact of the fault on the components. Situations of vulnerability due to a very high short-circuit current were highlighted for distribution networks supplied by high-power transformers (40- and 63-MVA classes), especially if operating at 15 kV.

The opportunity to add an FCL to avoid hazards caused by the fault was pointed out. Concerning power quality, the possibility of restricting, by means of an FCL, the area affected by a voltage dips following a polyphaser fault was pointed out. The impact of the FCL on DG was also investigated. It was pointed out that no need exists, in general, to reduce the contribution of the DG to the fault current. However, the possibility of using an FCL to avoid, in some particular cases, unwanted trips due to DG, thus increasing the DG power admissible for the network, was highlighted.

Finally, the possibility to interconnect, by means of an FCL, two distribution networks, thus increasing the short-circuit power without risking excessive vulnerability in case of fault, was discussed. The increased performance of the interconnected networks was quantitatively assessed in terms of maximum admissible disturbing power [6].

In this research, a comparative study of the breaker cut off behavior, voltage drop, voltage of the joint point and the transient behavior was performed in the presence of three types of resistive, inductive and bridge superconducting fault current limiter using the PSCAD / EMTDC software. A fixed speed wind turbines is equipped with an induction generator.

2. Proposed Superconducting Fault Current Limiter

Plenty of designs have been proposed for superconducting fault current limiter with different superconducting materials. The resistive superconducting fault current limiter is connected to the network only in series. An inductive superconducting fault current limiter was designed for a transformer with a superconducting secondary protection tube. Bridge Superconducting fault current limiter consists of a diode bridge and a superconductor as limiting agents.

A) The resistive superconducting fault current limiter

The resistive superconducting fault current limiter operates when the resistance increase at the time of superconductor suppression. The advantages of the resistive superconducting fault current limiter are its simple structure, small size and low capital cost in comparison with other types of superconductors.

During the normal operation, the superconductor is in its superconducting state, and the normal charge current passes theoretically without any loss. The circuit current rises sharply when short circuit happen, therefore in this case the superconductor goes under the transient condition at its normal state, so that a certain amount of non-linear resistance is generated as a self-inductance and self-trigger that limits the level of fault current.

In this study, a nonlinear resistive model was used to analyze the resistance characteristics of the superconducting fault current limiter sample with the PSCAD / EMTDC software. As the V-I curve shown in Fig. 1, the variation of the resistance is given by the slope of the curve [7 - 8].

B) The inductive superconducting fault current limiter model

In the inductive superconducting fault current limiter, the Cp capacitor is connected in parallel with the coil of limiter to simulate the distributed capacitor that appears in the winding. The distributed capacitor Cp has a much higher impedance than the LFCL inductance, which is the LFCL inductance impedance. Fig.2 represents the inductive superconducting fault current limiter studied in this research [9].

C) The bridge superconducting fault current limiter

Fig. 2 shows the three-phase bridge superconducting fault current limiter consisting of a series transformer superconductor coil and a diode bridge circuits. The diode bridge converts the three-phase AC to a DC current that flows through the superconductor coil. i_p and i_s are the current flow at the primitive and secondary coils of the transformer respectively, and in relation to the N transformer. They are as follows:

$$N = \frac{i_s}{i_p} \quad (1)$$

The short-circuit current (i_d) is almost equal to the highest secondary current:

$$i_d = \sqrt{2} i_s = \sqrt{2} N i_p \quad (2)$$

After charging the short circuit current is almost constant continuously, and it would be:

$$V_d = L_d \frac{di_d}{dt} = 0 \quad (3)$$

Therefore, the impedance observed on the primitive side of the transformer is very low. In fault status, the current increases with constant rate. The pre-phase current is given approximately by the following equation [10]:

$$i_{ph} = \frac{V_m}{L} (1 + i_0) (t - t_0) \cos(\omega t + \varphi) \quad t \geq t_0 \quad (4)$$

Where V_m is the amount of source voltage, L_D is the short-circuit inductance (as for the primitive side), t_0 is the moment the fault starts, φ is the phase angle and $i_0 = i(t_0)$.

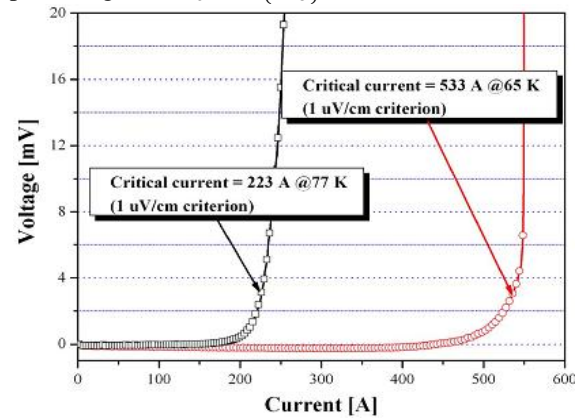


Fig. 1. V-I Curve limiting resistive fault current

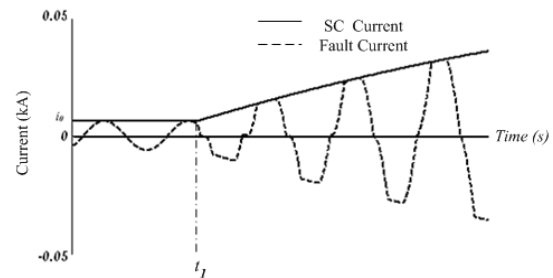


Fig. 2. Short circuit and fault current during fault and normal operation using a bridge type fault limiter

3. The Fixed Speed Wind Turbine Modeling

The Fixed speed wind turbines have the beneficial advantages like simplicity, powerfulness and reliability but they can hardly be controlled and have a high mechanical pressure, low power quality and high reactive power consumption [10-11]. Figure 3 shows the overall structure of the fixed speed wind turbine. The wind speed model, the wind turbine model, the mechanical propulsion model and induction generator are clarified in the following sections.

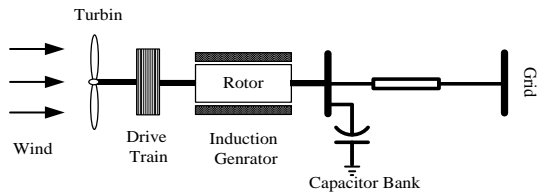


Fig. 3. The fixed speed wind turbine modeling Structure

A) Wind speed model

As illustrated in Fig. 4, the wind speed is modelled based on the sum of the base wind speed $V_{\omega a}(t)$, the rapid wind speed $V_{\omega r}(t)$, the gradient wind speed $V_{\omega g}(t)$ and the turbulent wind speed $V_{\omega t}(t)$ [12]. Considering these four types of wind speed, the preferred type for a single wind turbine is as follow:

$$V_{\omega}(t) = V_{\omega a}(t) + V_{\omega g}(t) + V_{\omega t}(t) + V_{\omega t}(t) \quad (5)$$

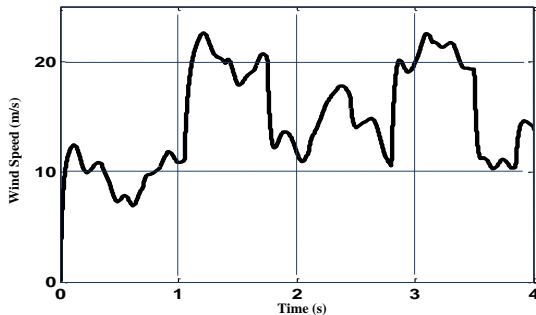


Fig. 4. Wind speed model

B) Wind turbine model

Generally, the relation between wind speed and mechanical energy driving from the wind can be described as follows [12-13]:

$$P_{\omega t} = \frac{\rho}{2} A_{\omega t} C_p(\lambda, \theta) V_{\omega}^3 \quad (6)$$

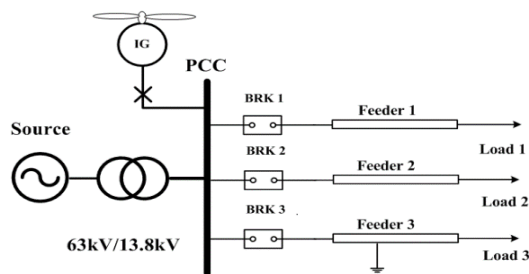


Fig. 5. Single-line view of the system examined

Where $P_{\omega t}$ is the power of wind energy (extracted mechanical power), ρ density of air, V_{ω} the wind speed, C_p is the power conversion coefficient which is a function of both tip speed ratio (λ), and blade pitch angle (β), $A_{\omega t} = \pi R^2$ the area covered by the rotor of the wind turbine, R the radius of the blade. ω_r rotational mechanical speed (rad/s) and λ are described as follows:

$$\lambda = R\omega_r/V_{\omega} \quad (7)$$

C) System shaft / propulsion model

The shaft model of wind turbine is defined by two-mass model, which is described by the following equations [12]:

$$\frac{\partial \theta_s}{\partial t} = \omega_t - \omega_g \quad (8)$$

$$\frac{\partial \omega_t}{\partial t} = \frac{1}{2H_t(T_t - K_s\theta_s + D(\omega_g - \omega_t))} \quad (9)$$

$$\frac{\partial \omega_g}{\partial t} = \frac{1}{2H_g(T_e - K_s\theta_s + D(\omega_g - \omega_t))} \quad (10)$$

Where:

T_t : the generator mechanical torque

T_e : the electromagnetic torque

H_t : the turbine blade inertia

H_g : the generator inertia

ω_t : the the turbine rotational speed

ω_g : the generator rotational speed

K : the shaft hardness

D : the damping constant

θ_s : the angular displacement between the two

Heads of shaft

D) Transient recovery voltage breaker

Fig 6. shows the transient recovery voltage breaker without installation of fault current limiter. The transient recovery voltage reaches a maximum of 15 kV in the absence of fault current limiter. Fig 7. shows the transient recovery voltage breaker using a resistive superconducting fault current limiter that in this case the transient recovery voltage reaches at the peak of 10 kV. Fig 8. shows the transient recovery voltage breaker using the inductive superconducting fault current limiter. The transient recovery voltage in this case reaches the maximum of 13 kV. Fig 9. shows the breaker recovery voltage using the bridge superconducting fault current limiter. The transient recovery voltage reaches over 15 kV.

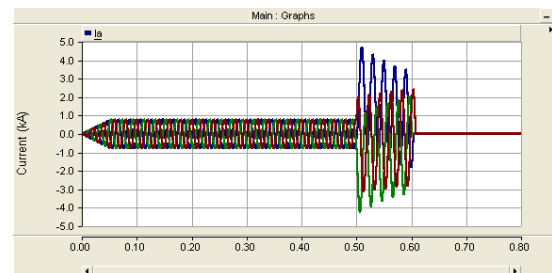


Fig. 6. Transient recirculation voltage circuit breaker without using Superconducting fault limit

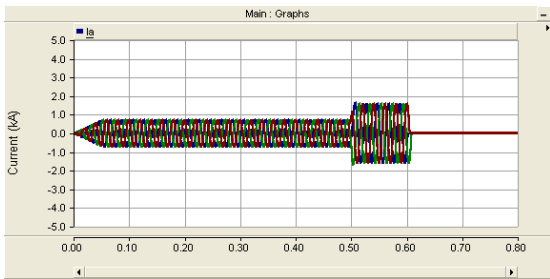


Fig. 7. Transient voltage recirculation circuit breaker using resistive superconducting fault current limiter

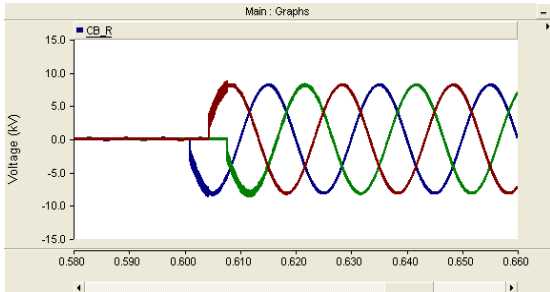


Fig. 8. Breaker of transient recovery voltage using resistive superconducting fault current limiter

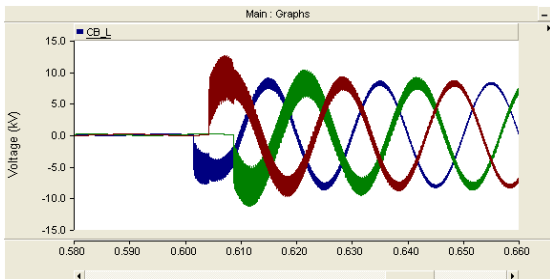


Fig. 9. Breaker of transient recovery voltage using induced superconducting fault current limiter

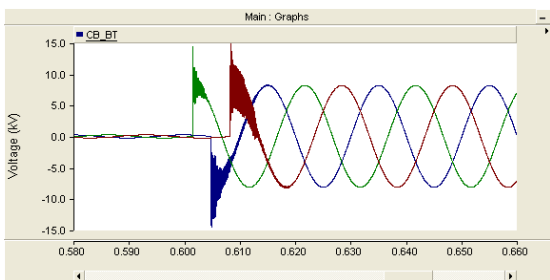


Fig. 10. Breaker of the transient recycle voltage using a bridge type superconducting fault current limiter

E) Current fault limiter

Fig 10. shows the flow path through the breaker functioning before zero current and without using fault current limiter. It is evident in Fig 10. that the fault current peak is about 5 kA, which can damage the equipment of system. Fig.11 shows the flow path through the breaker functioning before zero current and with using the resistive superconducting fault current limiter in which the fault current peak is about 1.8 kA. Using the resistive superconducting fault current limiter eliminates the asymmetric part of fault current. Fig 12. shows the flow path through the breaker

functioning before zero current and with using the inductive superconducting fault current limiter. In this part, the fault current value is about 1.6 kA. Fig 13. present the flow path through the breaker functioning before zero current with using the bridge superconducting fault current limiter. It is obvious when the fault current value is about 2.5 kA, the fault current increases steadily.

F) Voltage drop

Fig 14. presents the three-phase voltages of the earth joint point. It can be inferred from the picture that the voltage drops sharply up to 5% of the normal voltage after the short circuit. The voltage needs approximately one cycle to reach its natural value. Fig 15. shows the three-phase voltages of earth joint point using a resistive superconducting fault current limiter. As it shown in the picture, the voltage drop is reduced from 5% to 95% of the normal voltage after the short circuit. However, the transient voltage of the joint point increases. Fig 16. shows the three-phase voltages of earth junction point using the bridge superconducting fault current limiter. It can be clearly observed that the voltage drop is increased gradually after short circuit.

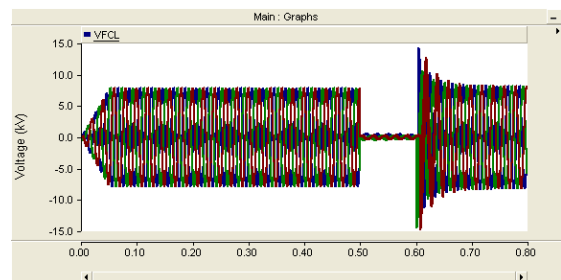


Fig. 11. PCC voltage without fault current limiter

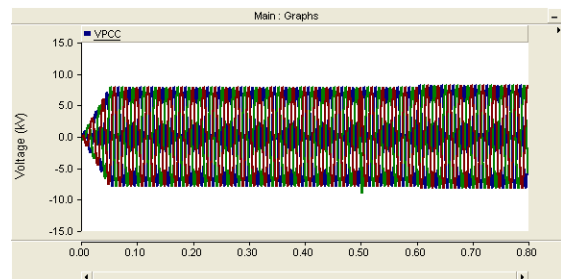


Fig. 12. PCC voltage using resistive fault current limiter

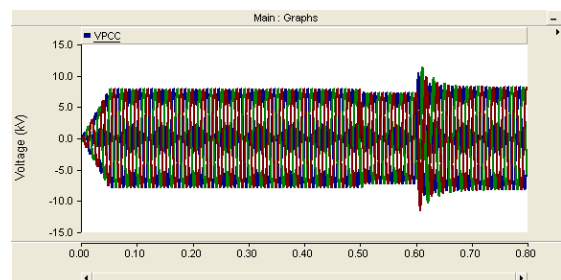


Fig. 13. PCC voltage using inductive fault current limiter

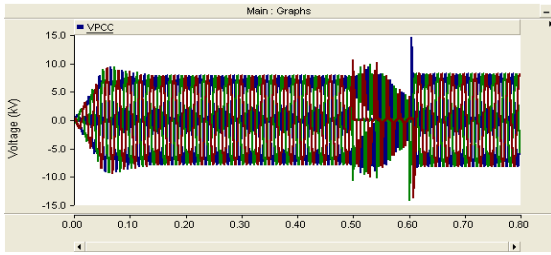


Fig. 14. PCC using a bridge type fault current limiter

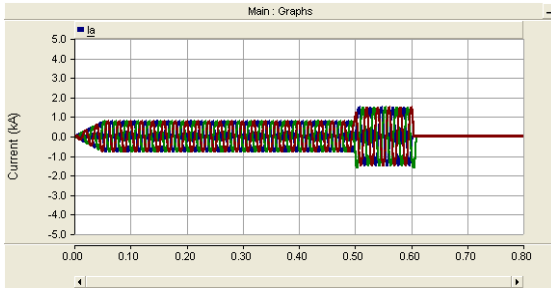


Fig. 15. Transient voltage recirculation circuit breaker using induced superconducting current fault limiter

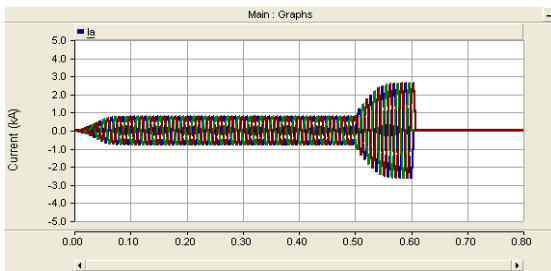


Fig. 16. Transient recirculation voltage circuit breaker using bridge suppressor of current fault limiter

G) *Transient stability of fixed wind turbines*

The three-phase short current fault in the feeder 3, which starts at $t = 10$ seconds, is simulated. After 100 milliseconds, the breaker separates the fault feeder. Fig 17. shows the speed of the induction generator rotor. As shown in that figure, all types of fault current limiter can provide more effective oscillations than the post-fault oscillations of the induction generator, but compared to the other cases the speed oscillation of the generator rotor in the bridge superconducting fault current limiter reduced effectively.

4. Simulation

The simulation was performed at $t = 0.6$ s along with the applied fault. Breaker has operated after 5 cycles. The total simulation time is 0.8 sec and the simulation steps responses are used 1μ s considering the breaker re-closed. The simulation parameters are listed in Table (1). The fault that was simulated in the feeder 3 of the system is presented in Fig 17.

Study 1: without fault current limiter in the system

Study 2: Using a resistive superconducting fault current limiter

Study 3: Using the inductive superconducting fault current limiter

Study 4: Using the bridge superconducting fault

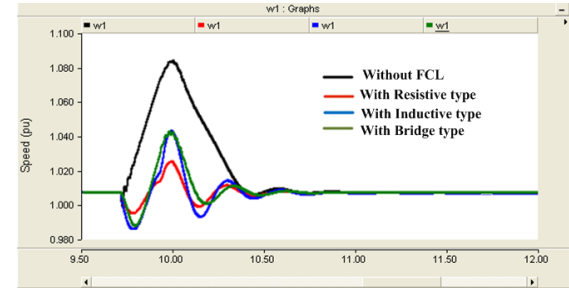


Fig. 17. Induction generator rotor speed in fault time

Table.1.
The simulation parameters are listed

Parameters		Value
Grid	Supply	63 kV
	Frequency	50Hz
	X/R ratio	8
Line	R	0.1(Ω /km)
	X	0.2(Ω /km)
	Length of feeder1 (F_1)	20 km
	Length of Feeder 2 (F_2)	20 km
Power	1 MW	
Voltage	690 V	
Frequency	50 Hz	
Number of poles	4	
Induction Generator	Slip	1/5%
	Power factor	0.9
	Stator resistance	0.006 Ω
	Stator reactance	0.08 Ω
	Rotor resistance	0.02 Ω
	Rotor reactance	0.1 Ω
	Magnetizing reactance	3 Ω

5. Conclusion

In this research, the effect of three types of superconducting fault current limiters on the transient recovery breaker voltage, drop voltage of the joint point, transient stability of fixed wind turbines has been investigated. The simulation results show that not only did the fault current limit but also the transient recovery voltage and the circuit breaker voltage and the joint point voltage have been effectively reduced using the bridge and resistive superconducting fault current limiters. The fault has increased. Also, with the help of a variety

of superconducting fault current limiters, the transient stability of limiter but the transient recovery voltage of the circuit breaker fixed wind turbines has been improved. Current restricted by the inductive superconducting fault current.

References

- [1] Lei Chen, Changhong Deng, Fang Guo, Yuejin Tang, Jing Shi, and Li Ren, "Reducing the Fault Current and Overvoltage in a Distribution System With Distributed Generation Units Through an Active Type SFCL," IEEE Transactions on Applied Superconductivity, vol.24, no.3, 2014.
- [2] Yu Zhao, Tapan K. Saha, Olav Krause, Yong Li, "Performance Analysis of Resistive and Flux-lock type SFCL in Electricity Networks with DGs," IEEE Power & Energy Society General Meeting, 2015.
- [3] Morandi, "Fault Current Limiter: An Enabler for Increasing Safety and Power Quality of Distribution Networks," IEEE Transactions on Applied Superconductivity, vol.23, no.6, 2013.
- [4] Sung-Hun Lim, Jae-Chul Kim, "Analysis on Protection Coordination of Protective Devices with a SFCL Due to the Application Location of a Dispersed Generation in a Power Distribution System," IEEE Transactions on Applied Superconductivity, vol.22, no.3, 2012.
- [5] Sung-Hun Lim, Jin-Seok Kim, Myong-Hyon Kim, and Jae-Chul Kim, "Improvement of Protection Coordination of Protective Devices through Application of a SFCL in a Power Distribution System with a Dispersed Generation," IEEE Transactions on Applied Superconductivity, vol. 22, no.3, 2012.
- [6] Hyung-Chul Jo, Sung-Kwan Joo, Kisung Lee, "Optimal Placement of Superconducting Fault Current Limiters (SFCLs) for Protection of an Electric Power System with Distributed Generations (DGs)," IEEE Transactions on Applied Superconductivity, vol. 23, no.3, 2013.
- [7] L. Z. Lin, K.P. Juengst, "Application studies of superconducting fault current limiter in electric power systems" IEEE Trans. Appl. Superconduct. 12,2002.
- [8] B. Gromoll, G. Ries, W. Schmidt, H.-P. Kraemer, B. Seebacher, B. Utz, R. Nies, H.-W. eumueller, E. Balzer, S. Fischer, and B. Heismann, "Resistive fault current limiters with YBCO films-100 kVA functional model," IEEE Trans. Appl. Superconduct., vol. 9,1999.
- [9] Lin Ye, K.P. Juengst, "Modeling and simulations of resistive type superconducting fault current limiter," IEEE Trans. Appl. Superconduct 14, 2004.
- [10] Lin Ye, K.P. Juengst, "Modeling and simulations of resistive type superconducting fault current limiter," IEEE Trans. Appl. Superconduct. 14,2004.
- [11] A. Gyore, A. Szalay, V. Sokolovsky, and W. Gawalek, "Improved design and system approach of a three phase inductive HTS fault current limiter for a 12 kVA synchronous generator," IEEE Trans. Appl. Superconduct., vol. 13, 2003.
- [12] M. T. Hagh and M. Abapour, "Nonsuperconducting Fault Current Limiter With Controlling the Magnitudes of Fault Currents," IEEE Trans. Power Electronics, Vol.24, 2009.
- [13] S. M. Muyeen, M. A. Mannan, M. H. Ali, R. Takahashi, T. Murata, and J. Tamura, "Stabilization of wind turbine generator system by STATCOM," IEEJ Trans. Power Energy, vol. 126, no.10 ,2006.